Original Article

FAM49B suppresses ovarian cancer cell growth through regulating MAPK signaling

Chen Yue^{1*}, Dong Zhou^{2*}, Yuzhao Zhou^{3*}, Qidong Feng^{3*}, Kun Fang⁴, Songshu Meng³, Weiting Yu⁵, Sha Du³, Dachuan Shen², Yifei Wang^{1,6}

¹Department of Obstetrics and Gynecology, Affiliated Zhongshan Hospital of Dalian University, No. 6 Jiefang Street, Dalian 116001, Liaoning, China; ²Department of Oncology, Affiliated Zhongshan Hospital of Dalian University, No. 6 Jiefang Street, Dalian 116001, Liaoning, China; ³Institute of Cancer Stem Cell, Dalian Medical University, No. 9 West Section, South Lvshun Road, Dalian 116044, Liaoning, China; ⁴Central Laboratory, Cancer Hospital of China Medical University, Cancer Hospital of Dalian University of Technology, Liaoning Cancer Hospital and Institute, Shenyang 110042, Liaoning, China; ⁵Central Laboratory, Affiliated Zhongshan Hospital of Dalian University, No. 6 Jiefang Street, Dalian 116001, Liaoning, China; ⁶Department of Obstetrics and Gynecology, The Second Affiliated Hospital of Dalian Medical University, Dalian 116027, Liaoning, China. *Equal contributors.

Received April 18, 2025; Accepted September 25, 2025; Epub September 25, 2025; Published September 30, 2025

Abstract: Recently, the family with sequence similarity 49 member B (FAM49B, also called CYRI-B) has garnered attention as a new target in cancer development. FAM49B is upregulated in ovarian cancer tissues; however, its role and mechanism in ovarian cancer progression remain unknown. Herein, we demonstrated that FAM49B knockdown significantly increases ovarian cancer cell viability, EdU incorporation, and clonogenic growth. In contrast, the forced expression of FAM49B achieved opposite effects. Furthermore, an ovo model was used to assess the in vitro effects of FAM49B depletion or overexpression on the growth of ovarian cancer. In a xenograft model, we observed that FAM49B overexpression alleviated tumor formation. Transcriptomic analysis of FAM49B-depleted and control cells revealed that FAM49B silencing upregulated the MAPK pathway. Consistent with the transcriptomic analysis results, we noted that FAM49B knockdown enhanced EGFR activation and downstream MEK-ERK signaling; in contrast, FAM49B overexpression exhibited opposite trends. In addition, FAM49B played a role in EGF-induced sphere growth of ovarian cancer cells. Notably, treatment with the MEK inhibitor trametinib considerably impaired the increased cell growth by FAM49B knockdown in cell culture and ovo models. Collectively, our results suggest that FAM49B can suppress the growth of ovarian cancer cells by regulating the MAPK signaling pathway.

Keywords: FAM49B/CYRI-B, ovarian cancer, MAPK, MEK, trametinib

Introduction

The protein family with sequence similarity 49 member B (FAM49B), also called CYFIP-related RAC interactor B, has recently been characterized as a novel regulator of actin dynamics by interacting with and suppressing the small GTPase RAC1 activity, thereby mediating multiple essential cellular functions, including T cell activation [1, 2], membrane protrusion, chemotaxis and cell migration [3-5]. FAM49B is highly expressed in many tumors and may play a role in tumor progression. However, both pro-tumor and tumor suppressor functions of FAM49B have been observed in certain tumors [6]. A study has revealed that FAM49B suppresses

tumor metastasis in pancreatic ductal adenocarcinoma (PDAC) by regulating tumor mitochondrial redox reactions and metabolism [7]. Using colorectal cancer and liver cancer cell models, another study revealed that FAM49B knockdown accelerated cell proliferation, suggesting the role of FAM49B as a tumor suppressor [8]. However, other studies have revealed that FAM49B plays an oncogenic role in breast, gallbladder, and gastric cancers [9-11]. Interestingly, while an in vivo study has suggested FAM49B as a tumor suppressor in live cancer [8], a recent study has revealed that FAM49B can promote liver tumor initiation in vivo [12]. Therefore, the biological function of FAM49B in cancer may be context-specific.

A recent study has revealed that FAM49B is upregulated in both ovarian cancer patient exosomes and cancer tissues [13], this suggests the role of FAM49B in ovarian cancer development. However, the putative role of FAM49B in ovarian cancer remains unknown.

Therefore, in the present study, we utilized gain-of-function and loss-of-function approaches and demonstrated that FAM49B inhibits ovarian cancer cell growth and tumor development. Furthermore, we provided evidence that the epidermal growth factor receptor (EGFR)-MAPK signaling pathway is involved in FAM49B-mediated effects on the growth of ovarian cancer cells. Overall, our findings suggest the tumor suppressor role of FAM49B in ovarian cancer progression.

Materials and methods

Cell culture and transfection

The human ovarian cancer cell lines, OVCAR-3 and Caov3 were obtained from the American Type Cell Culture (ATCC, Manassas, VA) and cultured according to ATCC guidelines. Hey-A8, PEO4, Hey, OVCAR-8, OVCAR-5, TOV-112D, COV504, ES-2, and KGN were kindly provided by Prof. Jing Tan (Sun Yat-sen University Cancer Center). Hey-A8 and PEO4 cell lines were cultured in DMEM (Gibco), Hey, OVCAR-8, OVCAR-5, OVCAR-3, TOV-112D, Caov3 and COV504 were cultured in RPMI-1640 (Gibco). All medium were supplemented with 10% FBS. All cell lines were maintained in an incubator at 37°C and 5% CO₂. Transfection of plasmids into all cells was performed using Lipofectamine 2000 (Invitrogen), according to the manufacturer's instructions.

Antibodies and reagents

The following antibodies were purchased from Cell Signaling Technology (America): antip-AKT S473 (4060S), Anti-P38 MAPK, anti-p-P38 MAPK (9215S), anti-p-SAPK/JNK (9251S), anti-SAPK/JNK (9252S). Anti-FAM49B (sc-390478) were purchased from SantaCruz (America). Anti-GAPDH (10494-1-AP), anti-Tubulin (11224-1-AP) and anti-Ki67 (27309-1-AP) were purchased from Proteintech (America). Anti-V5-Tag (AE101), anti-ERK1/2 (A4782), anti-p-ERK1/2 (AP0472), anti-P-C-JUN (AP0105) and anti-EGFR (A23381) were purchased

from Abclonal (China). Anti-P-EGFR (Tyr1068) (44-788G), goat anti-Rabbit IgG (H+L) (31460) and rabbit anti-Mouse IgG (H+L) (31480) were purchased from Invitrogen Thermo Fisher Scientific (America). Inhibitors Afatinib (S1011) and Erlotinib (targeting EGFR, S7786), PD-98059 (S1177) and Trametinib (targeting MEK1/2, S2673), SP600125 (targeting SAPK/JNK, S1460) and SB203580 (S1076) were purchased from Selleck (America). SP202190 (targeting p38MAPK, SP202190 HY-10295) was purchased from MCE (America). Drugs were dissolved in 0.5% dimethyl sulfoxide (DMSO) as stock solutions and stored at -20°C.

Lentiviral constructs and stable cell lines

FAM49B shRNA-1 (target sequence: GGATGT-ATGTTGTGTGTTT). FAM49B shRNA-2 (target sequence: AGATGAGAAGTTGCAAGAG), FAM-49B shRNA-3 (target sequence: CAGGTGAAT-GTAGTATTAA), FAM49B shRNA-4 (target sequence: CAATTACTATCTCATTTAT), FAM49B sh-RNA-5 (target sequence: CAATAACAATTCTGG-AATA) and non-coding shRNA were purchased from Thermo Scientific (America). Lentiviral particles were used to directly infect Hey, OVCAR-3, OVCAR-8 and TOV-112D cells and stable clones were selected using puromycin (Sigma), PCDNA3.1-3'V5 and FAM49B vectors were purchased from MiaoLing Plasmid Platform (China). V5-PCDH-FAM49B construct was generated in this study according to the standard molecular cloning procedures. Stable expression of FAM49B in Hey, OVCAR-3 and TOV-112D cell lines were established by using lentiviruses constructs expressing FAM49B.

Ethynyl deoxyuridine (EdU) incorporation assay

EdU Cell Proliferation Assay Kit with Alexa Fluor 555 (CO075S) was used to detect cell proliferation according to manufacturer's instructions. Briefly, cells were seeded in 96-well plates with complete media. 10 mM EdU was added to the plate and incubated for 2 h. Then, the cells were fixed, washed and stained with Hoechst 33342. The proportion of the cells incorporated EdU was determined with fluorescence microscopy.

Colony formation assay

For the clonogenic assay, cells were seeded in 6-well plates at 100 to 500 cells per well in trip-

licate wells. Three weeks later, cells were fixed with 4% paraformaldehyde in PBS, stained with 0.5% crystal violet, and photographed for counting the number of colonies (containing 50 or more cells) under light microscope, and colonies > 1 mm were counted using ImageJ software.

Spheroid formation assay

The assays were performed as previously described [14]. Ovarian cancer cells were trypsinized and plated at $(1 \times 10^3 \text{ cells/well})$ in ultra-low adhesion 96-well cell culture plates, providing with serum-deprived DMEM/F12 medium containing 20 ng/ml basic fibroblast growth factor (bFGF), 20 ng/mL of epidermal growth factor (EGF), and a proportion of B27 in medium (1:50 v/v) for 10 days. The reproduced 3D tumor microspheroids were detected and calculated by the inverted microscope.

Immunoblotting

The assays were performed as previously described [14, 15]. Briefly, cancer cells were harvested using RIPA lysis buffer (10 mM Tris-HCl, pH 8.0, 140 mM NaCl, 1 mM EDTA, 1% Triton X-100, 0.1% sodium deoxycholate, 0.1% SDS, pH 7.4) supplemented with a cocktail of protease and phosphatase inhibitors. Proteins were separated by polyacrylamide gel electrophoresis, subsequently transferred onto the nitrocellulose membrane. All membranes were blocked and incubated overnight by primary antibodies and subsequently incubated with anti-mouse or anti-rabbit secondary antibody.

Co-immunoprecipitation

Cells were harvested 24 hours after being transfected with plasmids in 1% Triton X-100 lysis buffer, which was supplemented with a mixture of protease and phosphatase inhibitors. Lysates were centrifuged and supernatants collected. A 50 μ L aliquot of the supernatants collected by centrifugation was taken for Inputs detection to evaluate the quality of procedure and the remaining supernatants was mixed with 30 μ l pre-washed protein G beads. Then, the pre-cleared supernatants collected by centrifugation were incubated with indicated antibody overnight at 4°C. Afterward, the mixture of protein and antibody were incubated with 30 μ l pre-washed G beads for 2 h at 4°C.

Immunoprecipitated complexes were washed five times with cold lysis buffer before boiling in 1X Loading Buffer. Immunoprecipitates and 2% lysate loading controls were then run on an SDS-PAGE gel and subsequent immunoblotting was conducted.

Immunofluorescence

Cells were plated on coverslips and treated as indicated. Cells were fixed with 4% paraformal-dehyde (PFA) for 20 minutes, permeabilized in 0.2% Triton X-100 for 15 min and incubated for 60 min in 3% Bovine Serum Albumin (BSA). Primary antibodies were diluted in blocking buffer and cells were incubated overnight at 4°C. Cells were washed with PBS and fluorescently labeled secondary antibodies were diluted in blocking buffer followed by incubation for 30 minutes at room temperature. Nuclei were stained with 5 μ g/mL DAPI (Sigma) in PBS. Images were acquired using a fluorescence microscope.

H&E staining and Immunohistochemical (IHC)

H&E staining and IHC were performed as reported in previous study [16]. Briefly, H&E staining was performed on 4 mm paraffin sections using a standard H&E staining protocol. Tissue sections were dewaxed using a decreasing xylene/alcohol series and then blocked with 3% BSA and incubated with anti-Ki67 and anti-FAM49B. The DAB Detection Kit was used to develop staining signal according to the protocols provided for the streptavidin-peroxidase system (Sangon Biotech, China). Hematoxylin was used for counterstaining. All sections were investigated by light microscopy.

In ovo chick embryo chorioallantoic membrane (CAM) model

Cancer cell growth in CAM assays was performed as described previously [16]. Briefly, 5×10^6 cancer cells were injected intravenously into the chicken CAM vein and then incubated at 37°C and 60% humidity for 6-8 days, images were taken.

In vivo tumor xenograft assay

All mice experiments were carried out under the Dalian Medical University's Institutional Animal Care and were approved by the Laboratory Animal Ethics Committee of Dalian Medical University (Approval Number: AEE-23027). Total 20 female nude mice (5-6 weeks) were obtained from the Beijing Vital River Laboratory Animal Technology Co., Ltd. and divided into four groups randomly (n=5 per group). Animals were four maintained in the specific pathogen-free facility with standard 12 h light/dark cycles, allowed chow and water ad libitum, and euthanized humanely in their home cages with ${\rm CO_2}$ followed by cervical dislocation.

To assess subcutaneous tumor growth, female BALB/c nude mice were subcutaneously inoculated in the right dorsal flank total 10 female nude mice (5-6 weeks) were divided into two groups randomly (n=5 per group) and each mouse was injected with FAM49B-overexpressing TOV-112D or control cells (5 × 106 cells in 100 µL PBS/mouse) to induce tumor development and measure tumor volume every three days. After 4 weeks, the mice were euthanized, and tumors were surgically removed from mice. The tumors were measured using a caliper and their volume was calculated using the following formula: π (width² × length)/6 (mm³). Tumors were harvested 5 weeks post inoculation, fixed in 10% neutral buffered formalin (NBF), embedded in paraffin, sectioned, and stained with hematoxylin and eosin (H&E). Immunohistochemical (IHC) staining was performed with antibodies.

Statistical analysis

Statistical analysis was performed using GraphPad Prism 9.0 (GraphPad Software, USA), and the outcomes are displayed as the means \pm standard error of the mean (SEM). Unpaired two-tailed t-tests were employed for statistical comparisons between the two groups. For datasets with more than two groups, a one-way ANOVA was performed, followed by Tukey's post hoc test. Results were considered as statistically significant at **P < 0.01, ***P < 0.0001.

Results

FAM49B suppresses ovarian cancer cell growth in vitro

First, we investigated the relationship between FAM49B expression and overall survival in

patients with ovarian cancer using gene expression data from multiple datasets (https:// kmplot.com/analysis/). FAM49B expression analysis in patients with ovarian cancer using the Kaplan-Meier methods revealed that patients with low FAM49B expression had a relatively, although not significantly, decreased overall survival compared with patients with high FAM49B expression (Figure 1A). Next, we examined the biological role of FAM49B in ovarian cancer progression. We used immunoblotting (IB) to measure FAM49B protein levels in various ovarian cancer cell lines, which indicated a varied expression pattern (Figure 1B). Therefore, we stably knocked down FAM49B in Hey, OVCAR-3, OVCAR-8, and TOV-112D cell lines by transducing with lentiviral particles encoding either FAM49B-specific short hairpin RNAs (shRNAs) or a nontarget control (shControl). IB was used to confirm the knockdown efficiency (Figure 1C). In addition, we stably overexpressed FAM49B in Hey, OVCAR-3, and TOV-112D cell lines by transducing with lentiviruses packaged with either a full-length human FAM49B cDNA or an empty vector. IB confirmed the ectopic expression of FAM49B in these cell lines (Figure 1D). Then, these established cell lines, with either knockdown or overexpression of FAM49B, were used to evaluate cell growth and proliferation via CCK-8, EdU staining, and clonogenic growth assays. Compared with the matched shRNA controls, the stable depletion of FAM49B in Hev and OVCAR-8 cells significantly increased cell viability (Supplementary Figure 1A, CCK-8 assay), EdU incorporation (Supplementary Figure 1B), and clonogenic growth (Figure 1E, colony formation assay). To confirm that FAM49B deficiency resulted in the inhibition of growth or proliferation of FAM49B shRNAinfected ovarian cancer cells, a rescue experiment was performed by restoring FAM49B expression by transfecting with a cDNA encoding FAM49B. Figure 1F illustrates that restoration of FAM49B expression significantly rescued the inhibitory effects of FAM49B knockdown on clonogenic growth. To compare with knockdown experiments, gain-of-function studies were performed. FAM49B overexpression in Hey and TOV-112D cells decreased cell growth or proliferation (Figure 1G, clonogenic growth assay; Supplementary Figure 1C and 1D, CCK-8 and EdU assays, respectively), exhibiting an opposite effect to FAM49B knockdown.

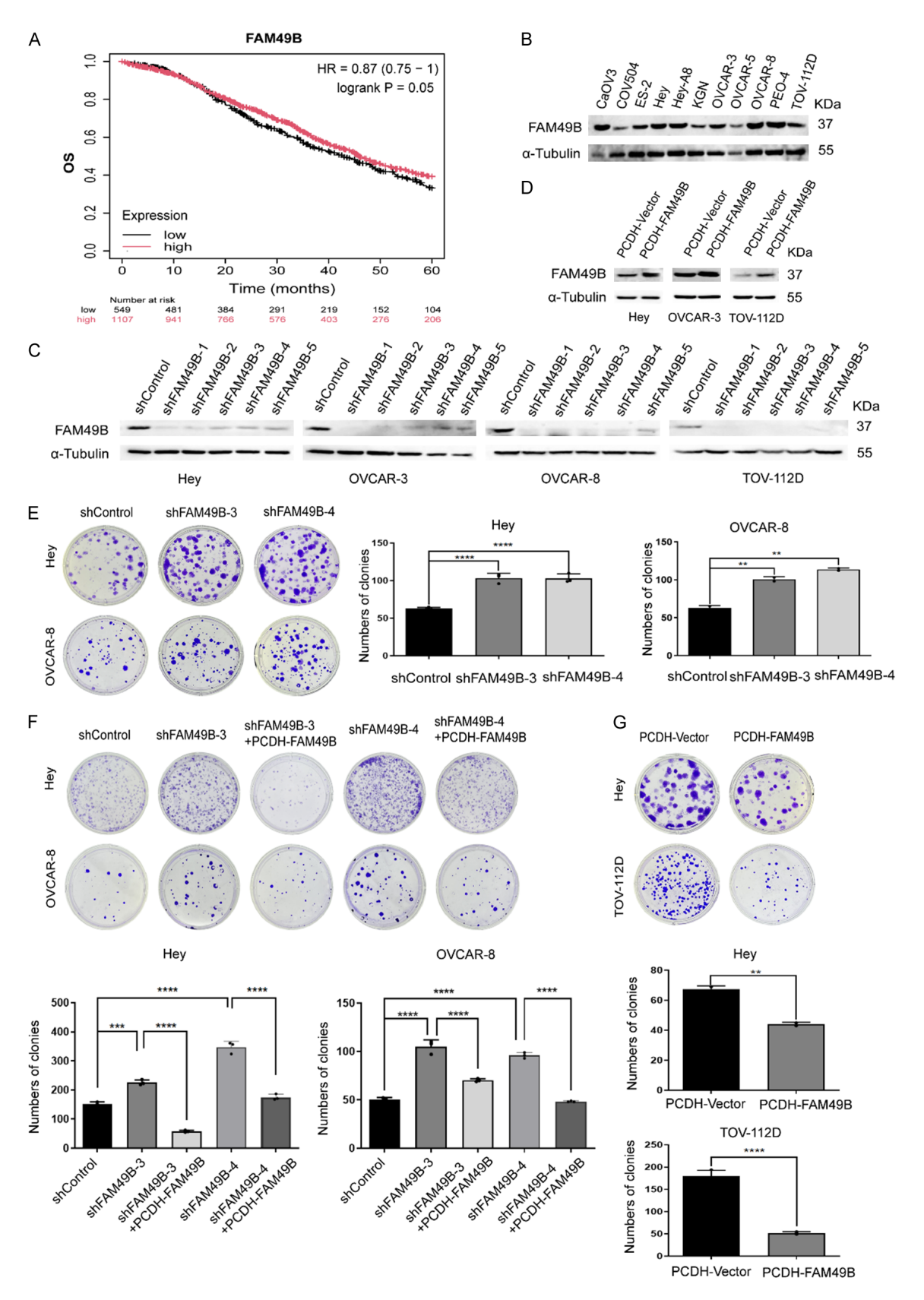


Figure 1. FAM49B expression inhibits ovarian cancer cell growth. (A) Kaplan-Meier overall survival (OS) of patients created using Kaplan-Meier Plotter network. Patients were classified into FAM49B high and FAM49B low subgroups

and analyzed as indicated. (B) Immunoblotting (IB) analyses of the abundance of FAM49B protein in different ovarian cancer cell lines. α -Tubulin was used as a loading control. (C, D) IB analysis of FAM49B protein levels in the ovarian cancer cell lines Hey, OVCAR-3, OVCAR-8, and TOV-112D after the stable knockdown of FAM49B expression using lentivirus approaches (C), and Hey, OVCAR-3, and TOV-112D cells with stable FAM49B expression via lentivirus approaches (D). (E, F) Representative images and quantification of the clonogenic growth of Hey and OVCAR-8 cells with FAM49B knockdown (E), or rescued by restoring FAM49B expression in these FAM49B knockdown cells (F). (G) Representative images and quantification of the clonogenic growth of Hey and TOV-112D cells with stable FAM49B expression. All experiments were performed in triplicate. All statistical data were presented as Mean \pm SD (**P < 0.01, ***P < 0.001, ****P < 0.0001).

FAM49B inhibits ovarian cancer growth in ovo and in a xenograft mouse model

After confirming that elevated FAM49B expression suppresses ovarian cancer growth in vitro. we assessed the effects of FAM49B on tumor growth in an ovo model, which has been successfully constructed and utilized in our previous studies [17-19]. Either FAM49B-depleted Hey and OVCAR-8 or FAM49B-overexpressing Hey and TOV-112D cells and their respective control cells were implanted on the chorioallantoic membrane (CAM) of chicken embryos on embryonic day 10. We observed that FAM49B knockdown increased the number and size of tumors in the CAM model compared to control cells (Figure 2A); in contrast, FAM49B overexpression achieved an opposite result (Figure 2B).

Next, we investigated the tumor-suppressive role of FAM49B in a xenograft model. For this, FAM49B-overexpressing TOV-112D or control cells were subcutaneously injected into nude mice, and tumor growth and weight were monitored. Compared with control mice, tumor growth, weight, and volume were significantly decreased in mice bearing FAM49B-overexpressing cells (Figure 2C-E). Histologic examination via hematoxylin and eosin (H&E) staining confirmed the presence of tumors (Figure **2F**). In addition, Immunohistochemical (IHC) analysis revealed a decrease in Ki-67-positive cells in the FAM49B-overexpressed tumors compared with control tumors (Figure 2F). As expected, IHC staining confirmed the high levels of FAM49B in FAM49B-overexpressed tumors (Figure 2F).

FAM49B downregulates EGFR-MAPK signaling pathway

To determine how FAM49B exerts its proposed tumor suppressor function, we subjected parental OVCAR-8 and FAM49B-depleted

OVCAR-8 cells to RNA-Seq analysis (GEO accession number: GSE290202, Supplementary Table 1). Volcano plot analysis revealed that 205 genes were upregulated and 843 genes were downregulated after FAM49B knockdown (Figure 3A). KEGG analysis revealed that the differentially expressed genes were significantly enriched in the MAPK pathway (Figure 3B). The enriched genes, which appeared to be associated with the EGFR-MAPK signaling pathway, were further visualized using a clustered heatmap of RNA-Seq analysis (Figure 3C). Consistent with the RNA-Seg results, the phosphorylation levels of EGFR (pY1068, an indicator of EGFR activation), mitogen-activated protein kinase (MEK), the major MAPK pathway components (ERK1/2, JNK, and p38 MAPK), and C-JUN (S63) were markedly increased in FAM49B-depleted Hey and OVCAR-3 cells compared with control cells (Figure 3D). In contrast, FAM49B overexpression in Hey and TOV-112D cells exhibited opposite trends (Figure **3E**). Of note, while the phosphorylation levels of AKT (S473) were not noticeably changed after FAM49B knockdown (Figure 3D), FAM-49B overexpression strongly downregulated AKT phosphorylation (Figure 3E). Rescue experiments were conducted to further confirm the effect of FAM49B knockdown on EGFR-MAPK activation. The ectopic expression of FAM49B in FAM49B-depleted Hey and OVCAR-3 cells partially weakened the increased activation of EGFR, MAPK, and C-JUN induced by FAM49B knockdown (Figure 3F). Collectively, our findings suggest that FAM49B downregulates the EGFR-MAPK pathway in ovarian cancer cells.

To elucidate the underlying mechanisms by which FAM49B regulates the EGFR-MAPK pathway, we determined whether FAM49B interacts with EGFR in ovarian cancer cells. Co-immunoprecipitation (co-IP) experiments revealed both exogenous and endogenous interaction between FAM49B and EGFR in Hey

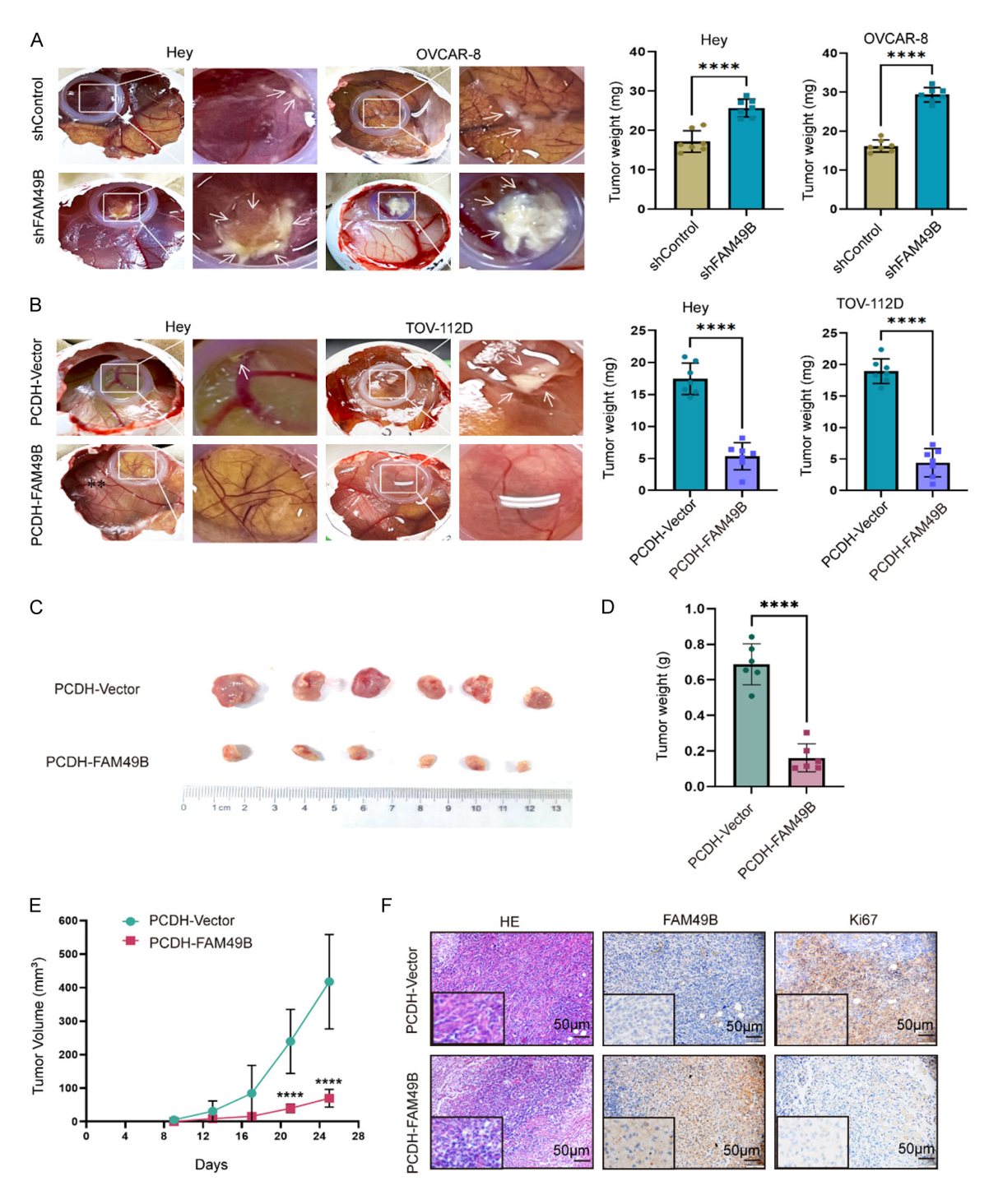


Figure 2. Evaluation of the effects of FAM49B expression on tumor growth in ovo and in a xenograft mouse model. (A, B) Effects of FAM49B knockdown (A) or overexpression (B) on tumor growth were evaluated in a chick embryo chorioallantoic membrane (CAM) model. For each embryo, 5.0×10^6 cells were inoculated. A minimum of ten embryos per condition was analyzed and representative images were shown. Arrows indicate tumor. Tumor weights (mg) after excision from the CAM (upon experiment termination on the 10th day). Data show mean \pm SEM (n=7). (C) FAM49B-ovexpressing TOV-112D and control cells were subcutaneously injected into mice, and tumor images are shown. (D, E) Tumor weight (D) and volume (E) of mice were determined. (F) Representative images of H&E staining and immunohistochemical staining for Ki67 and FAM49B in tumor sections. The magnification of the images is $400 \times$, scale bar, $50 \ \mu m$. All statistical data were presented as Mean \pm SD (****P < 0.0001).

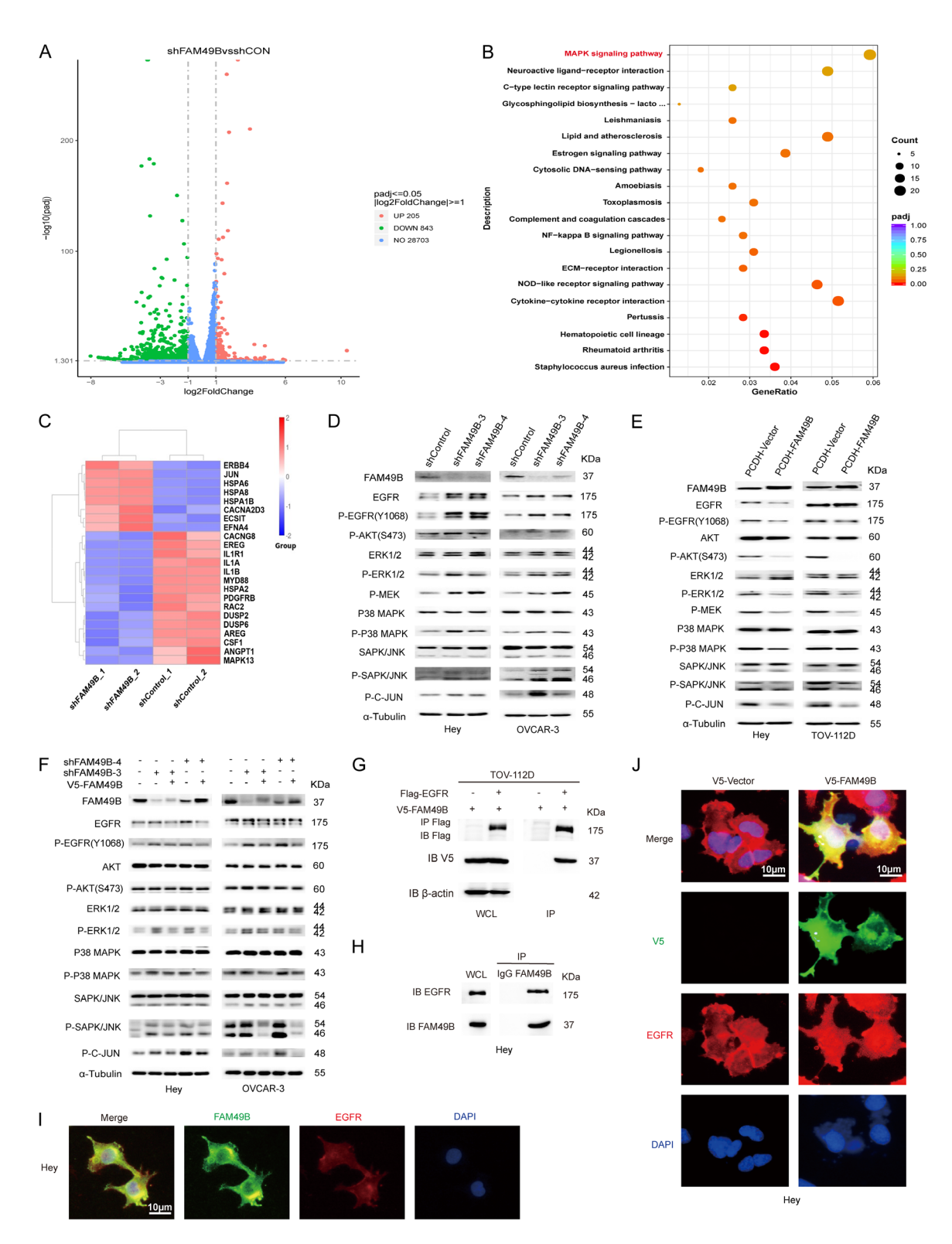


Figure 3. FAM49B expression regulates EGFR activation and ERK-MAPK pathway. (A) Volcano plot showing the RNA-Seq analysis results of differentially expressed genes between FAM49B-depleted and control OVCAR-8 cells. (B) KEGG enrichment analysis for the differentially expressed genes after FAM49B knockdown. (C) Clustered heatmap visualization of the differentially expressed genes between shFAM49B and shControl OVCAR-8 cells; the color bar denotes Z-score normalized TPM (Transcript Per Million) expression value. (D, E) Immunoblotting (IB) analyses of the phosphorylation levels of EGFR, MEK, ERK, JNK, p38MAPK, C-JUN, and AKT in FAM49B-silenced Hey and OVCAR-3 cells (D) and FAM49B-overexpressing Hey and TOV-112D cells (E). (F) IB analysis in FAM49B-silenced Hey and OVCAR-3 cells, with FAM49B rescuing the knockdown effects. All experiments were performed twice, and representa-

tive images were shown. In all IB experiments, α -Tubulin was used as a loading control. (G) Immunoprecipitation followed by IB analyses of interaction between Flag-tagged EGFR and V5-tagged FAM49B in transfected TOV-112D cells. (H) Immunoprecipitation followed by IB analyses of interaction between endogenous EGFR and FAM49B in Hey cells. (I) Immunofluorescence staining detection of colocalization between endogenous EGFR and FAM49B in Hey cells. DAPI was used for nuclear staining. The magnification of the images is 1000° , scale bar, $10~\mu m$. (J) Immunofluorescence staining detection of colocalization between endogenous EGFR and V5-FAM49B in transfected Hey cells. DAPI was used for nuclear staining. The magnification of the images is 1000° , scale bar, $10~\mu m$.

cells or transfected TOV-112D cells (**Figure 3G** and **3H**). Consistent with co-IP results, immunofluorescence imaging revealed the co-localization of FAM49B and EGFR in transfected Hey cells (**Figure 3I** and **3J**).

FAM49B plays a role in EGF-induced growth of ovarian cancer cells

After confirming that FAM49B expression downregulates the EGFR-MAPK signaling pathway, we hypothesized whether FAM49B regulates the EGFR-MAPK signaling pathway in response to epidermal growth factor (EGF) stimulation. For this, FAM49B-ovexpressing Hev and control cells were stimulated with EGF; IB was used to monitor the activation of the EGFR-ERK pathway. Figure 4A illustrates that FAM49B overexpression in Hey cells markedly attenuated EGFR and ERK1/2 activation approximately 30 min after EGF treatment, compared with control cells. Furthermore, EGFinduced AKT activation was strongly attenuated in FAM49B-overexpressing cells. Similar findings were noted in EGF-stimulated TOV-112D cells following manipulation of FAM49B expression (Figure 4B). EGF can promote cancer cell growth and is an important growth factor for establishing three-dimensional (3D) sphere cultures.

We cultured FAM49B-overexpressing Hey and TOV-112D cells, along with their respective controls, in non-adherent, serum-free conditions supplemented with EGF, bFGF, and B27. To avoid aggregate formation, sub-cultured spheroids were used throughout the study. FAM49B overexpression resulted in smaller spheres compared to controls (Figure 4C). In contrast, FAM49B-depleted Hey and OVCAR-8 cells formed larger spheres than control cells (Figure 4D).

MEK inhibitor Trametinib antagonizes the effect of FAM49B knockdown on ovarian cancer cell growth

Our abovementioned findings suggest the essential role of the EGFR-MAPK pathway in

FAM49B-mediated effects on ovarian cancer cell growth. Next, we investigated whether the pharmacological inhibition of the EGFR-MAPK pathway reverses the increased cell growth after FAM49B knockdown. For this, we used the following inhibitors: afatinib and erlotinib (targeting EGFR), PD98059 and trametinib (targeting MEK1/2), SP600125 (targeting SAPK/ JNK), and SB203580 and SP202190 (targeting p38MAPK). To prevent cytotoxicity, the effective concentrations of these inhibitors were selected via a dose-response assay for each inhibitor (data not shown). We confirmed the inactivation of the target pathways in Hey cells using specific inhibitors at given concentrations for 24 h (Figure 5A). Notably, among the inhibitors tested, trametinib completely inhibited the increased phosphorylation of ERK1/2 after FAM49B knockdown and the basal phosphorylation of ERK1/2 in control cells (Figure 5A). Consistently, treatment with trametinib, but not other inhibitors, significantly impaired increased colony formation in both Hey and TOV-112D cells with FAM49B knockdown (Figure 5B). Furthermore, trametinib treatment suppressed tumor growth in FAM49B-depleted Hey and OVCAR-8 cells in the ovo model (Figure 5C).

Discussion

In the present study, we first reported that FAM49B acts as a tumor suppressor in ovarian cancer. Mechanistically, FAM49B inhibits ovarian cancer cell growth partially by downregulating the EGFR-MAPK signaling pathway. Therefore, our findings may reveal the role and mechanism of action of FAM49B in the progression of ovarian cancer.

FAM49B (also known as CYRI-B) has recently garnered attention as a new target in cancer development [6]. However, recent studies have revealed a complex, even paradoxical, role of FAM49B in cancer, as it can either promote or suppress tumor progression in specific contexts [6]. Particularly in the case of PDAC, while

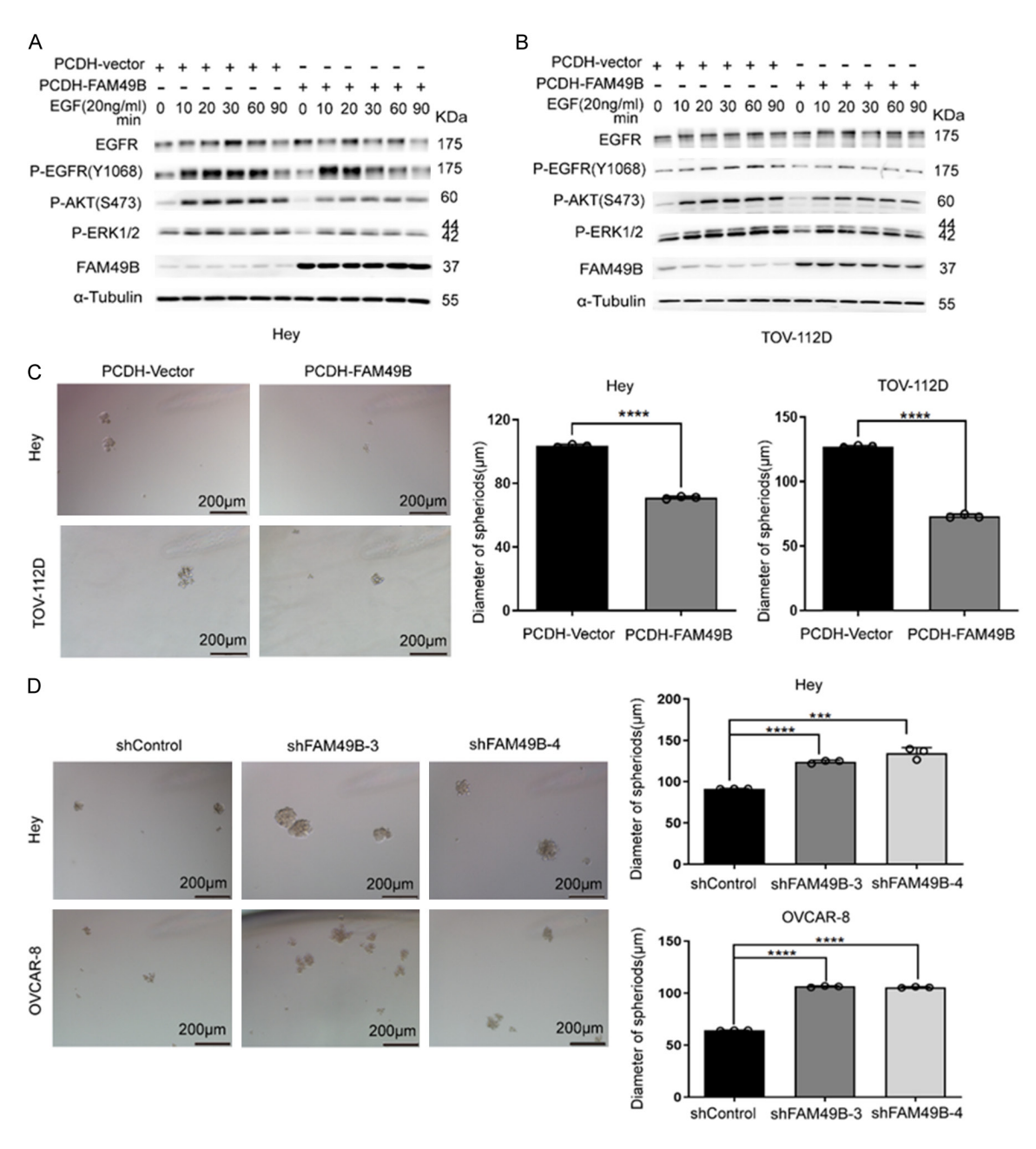


Figure 4. FAM49B expression attenuates EGF-induced sphere growth. (A, B) Immunoblotting (IB) analyses of the phosphorylation levels for EGFR, ERK, and AKT in FAM49B-overexpressing Hey (A) and TOV-112D (B) cells upon exposure to EGF (20 ng/ml) for the indicated time. α-Tubulin was used as a loading control. (C, D) Representative images of three-dimensional (3D) spheres of FAM49B-overexpressing Hey and TOV-112D cells (C) and FAM49B-depleted Hey and OVCAR-8 cells (D). The magnification of the images is 100×, scale bars, 200μm. Sphere diameter was determined and quantified. All statistical data were presented as Mean \pm SD (***P< 0.001, ****P< 0.0001).

FAM49B serves as a suppressor of cancer cell proliferation and invasion by regulating tumor mitochondrial redox reactions and metabolism [7], another study has revealed that loss of FAM49B can inhibit metastasis during PDAC progression [6]. Notably, FAM49B deficiency enhanced early PDAC progression [6], suggest-

ing that FAM49B acts as a tumor suppressor in early stages of PDAC but exhibits a pro-meta-static function in late stages of PDAC. Therefore, the role of FAM49B in cancer development may be complex, and researchers should be cautious when defining its role in distinct cancer contexts.

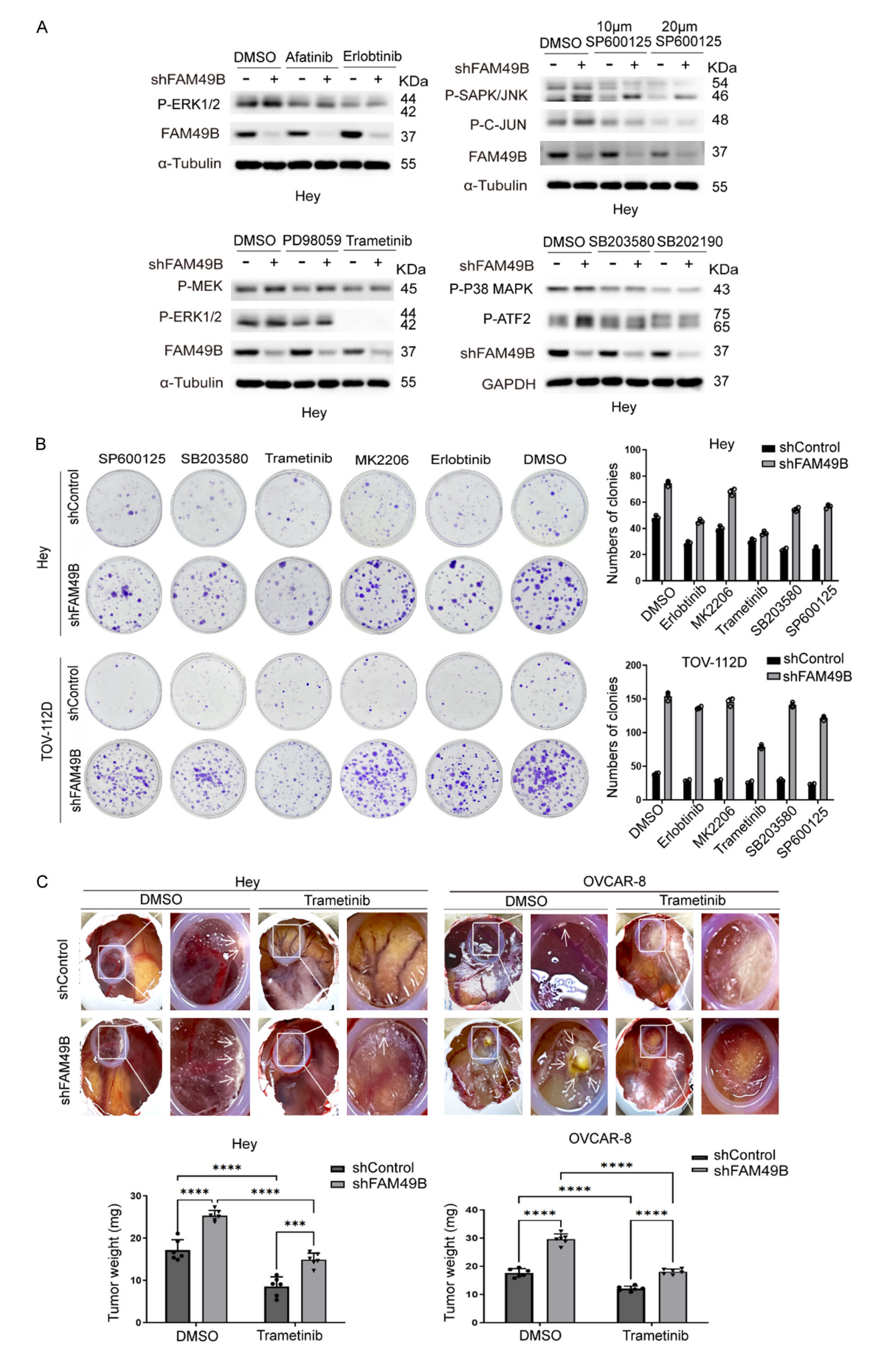


Figure 5. MEK inhibitor Trametinib antagonizes FAM49B-knockdown-induced cell growth. A. Immunoblotting detection of the phosphorylation of MEK1/2, ERK1/2, JNK, and p38MAPK in Hey cells upon exposure to indicated inhibitors for 24 h. PD98059 and Trametinib (10 μM/mL), SP600125 (10, 20 μM/mL), SB203580 and SB202190 (10 μM/mL). α-Tubulin was used as a loading control. B. Representative images and quantification of clonogenic growth of FAM49B-depleted Hey and TOV-112D cells treated with indicated inhibitors. C. Effect of the MEK inhibitor trametinib on tumor growth in an ovo model. Arrows indicate tumor presence. Tumor weights (mg) after excision from the CAM (upon experiment termination on the 10th day). Data show mean ± SEM (n=6). All statistical data were presented as Mean ± SD (****P<0.0001).

In addition to the complex role of FAM49Bb in the tumorigenesis and development of PDAC, different studies have revealed distinct differences in FAM49B expression in PDAC progression. While one study has revealed the downregulation of FAM49B expression in PDAC cells by the tumor microenvironment [7], another study has revealed high FAM49B expression in pancreatic tumors in a mouse model of KRAS and p53-driven pancreatic cancer [6]. Considering that FAM49B is upregulated in ovarian cancer tissues [13], one may speculate the oncogenic role of FAM49B in ovarian cancer. However, in the present study, using gain and loss-of-function experiments and cell cultures, an ovo CAM model, and a mouse model, we demonstrated that FAM49B suppresses ovarian cancer cell growth. This suggests the tumor suppressor role of FAM49B in ovarian cancer. Therefore, there are inconsistencies between high FAM49B expression in ovarian cancer tissues noted in a previous study and the anti-growth effect of FAM49B noted in our study. In addition, whether FAM49B expression exerts an effect on the motility of ovarian cancer cells remains unknown. This should be investigated in further studies because it can provide sufficient evidence for the role of FAM49B in ovarian cancer progression.

To date, the mechanisms of action of FAM49B in certain cancers have been partially explored. As expected, FAM49B, as a newly identified RAC1 interactor, negatively regulates RAC1 activity and signaling, thereby suppressing PDAC tumorigenesis [6]. Interestingly, the FAM49B-RAC1 axis acts downstream of LanClike protein-1 to promote liver tumor initiation by suppressing the Rac1-NADPH oxidase-driven reactive oxygen species production [12]. In addition to regulating RAC1 activity and signaling, other mechanisms of action of FAM49B in cancer have been documented. A recent study revealed that FAM49B stabilizes ELAVL1 protein and regulates the downstream Rab10/ TLR4 pathway, thereby promoting breast cancer progression [10]. Another observation suggests that FAM49B impairs macropinocytic uptake of the lysophosphatidic acid receptor 1. thereby promoting PDAC metastasis [6]. In addition, FAM49B can suppress PDAC progression by regulating tumor mitochondrial redox reactions and metabolism [7]. Overall, these studies suggest that the mechanisms of action of FAM49B in cancer are not limited to regulating RAC1 activity and signaling. In the present study, we demonstrated that elevated FAM49B expression downregulates the ERK-MAPK signaling pathway in ovarian cancer cells. Our findings are consistent with those of a previous study, which revealed that during the early stages of PDAC development, FAM-49B deletion enhanced ERK and JNK-induced proliferation in precancerous lesions [6]. Moreover, we observed that the MEK inhibitor trametinib can counteract the effect of FAM49B knockdown on ovarian cancer cell growth, supporting the notion that the ERK-MAPK pathway plays a role in FAM49B-mediated effects on ovarian cancer cell growth.

EGFR is overexpressed in more than 50% of patients with ovarian cancer and is associated with poor clinical outcomes [20-25]. EGFR signaling promotes ovarian tumorigenesis, including proliferation, migration, and angiogenesis [26]. Moreover, several EGFR inhibitors, including erlotinib, have been tested in clinical trials [27, 28]. However, current studies have revealed that patients with ovarian cancer exhibit a limited benefit from the EGFR inhibitors, namely, erlotinib or afatinib [29-31]. The complex regulation of EGFR signaling in ovarian cancer can contribute to the undesirable effects of these EGFR inhibitors. In the present study, we reported that FAM49B knockdown enhanced EGFR activation under basal conditions; in contrast, FAM49B overexpression markedly attenuated EGFR and ERK1/2 activation upon EGF treatment. Collectively, our study findings suggest that FAM49B is a novel regulator of EGFR signaling in ovarian cancer. It should be

noted that in our study both EGFR inhibitors Afatinib and Erlotinib did not attenuate the phenotypes induced by FAM49B knockdown effectively as Trametinib did. Previous studies have documented that ovarian cancer might express ERBB2 and/or ERBB3, which activate the MAPK signaling as did EGFR [32-34]. As both Afatinib and Erlotinib effectively target EGFR but not ERBB2/3, the activated MAPK pathway by ERBB2/3 might not be inhibited sufficiently by Afatinib or Erlotinib. Trametinib effectively targets MEK1/2 [35], which is downstream of EGFR and/or ERBB2/3 signaling pathways. This might explain partially that compared to Afatinib and Erlotinib, Trametinib treatment achieved more potent inhibitory effects on cell growth. Further studies should be performed to examine the expression of ERBB2/3 in the tested ovarian cancer cell lines.

Conclusions

We demonstrated the anti-growth role of FAM49B in ovarian cancer. Furthermore, our findings suggest FAM49B as a new negative regulator of EGFR activity, with potential clinical implications in EGFR-driven ovarian cancer.

Acknowledgements

This work was supported by grants from Department of Science & Technology of Liaoning province (Liaoning Provincial Science and Technology Joint Program Project, Natural Science Foundation-Doctoral Research Start-up Project, 2024-BSLH-005 to CY), and Liaoning Provincial Natural Science Foundation General Program (2025-MS-248 to SD), and from Affiliated Zhongshan Hospital of Dalian University (DLDXZSYY-KYQD202209Z to YW), and by Dalian medical scientific research projects (2311034 to DZ).

Disclosure of conflict of interest

None.

Address correspondence to: Yifei Wang, Department of Obstetrics and Gynecology, The Second Affiliated Hospital of Dalian Medical University, Dalian 116027, Liaoning, China. Tel: +86-411-84671291-5109; Fax: +86-411-84671291-5109; E-mail: yangduo@dlut.edu.cn; Dachuan Shen, Department of Oncology, Affiliated Zhongshan Hospital of Dalian University, No. 6 Jiefang Street,

Dalian 116001, Liaoning, China. Tel: +86-411-6289-3627; Fax: +86-411-6289-3627; E-mail: shendachuan@dlu.edu.cn; Sha Du, Institute of Cancer Stem Cell, Room 415, Dalian Medical University, No. 9 West Section, South Lvshun Road, Dalian 116044, Liaoning, China. Tel: +86-411-8611-0496; Fax: +86-411-8611-0496; E-mail: dusha@dmu.edu.cn

References

- [1] Shang W, Jiang Y, Boettcher M, Ding K, Mollenauer M, Liu Z, Wen X, Liu C, Hao P, Zhao S, McManus MT, Wei L, Weiss A and Wang H. Genome-wide CRISPR screen identifies FAM49B as a key regulator of actin dynamics and T cell activation. Proc Natl Acad Sci U S A 2018; 115: E4051-E4060.
- [2] Park CS, Guan J, Rhee P, Gonzalez F, Lee HS, Park JH, Coscoy L, Robey EA, Shastri N and Sadegh-Nasseri S. Fam49b dampens TCR signal strength to regulate survival of positively selected thymocytes and peripheral T cells. Elife 2024: 13: e76940.
- [3] Fort L, Batista JM, Thomason PA, Spence HJ, Whitelaw JA, Tweedy L, Greaves J, Martin KJ, Anderson KI, Brown P, Lilla S, Neilson MP, Tafelmeyer P, Zanivan S, Ismail S, Bryant DM, Tomkinson NCO, Chamberlain LH, Mastick GS, Insall RH and Machesky LM. Fam49/CYRI interacts with Rac1 and locally suppresses protrusions. Nat Cell Biol 2018; 20: 1159-1171.
- [4] Yuki KE, Marei H, Fiskin E, Eva MM, Gopal AA, Schwartzentruber JA, Majewski J, Cellier M, Mandl JN, Vidal SM, Malo D and Dikic I. CYRI/FAM49B negatively regulates RAC1-driven cytoskeletal remodelling and protects against bacterial infection. Nat Microbiol 2019; 4: 1516-1531.
- [5] Kaplan E, Stone R, Hume PJ, Greene NP and Koronakis V. Structure of CYRI-B (FAM49B), a key regulator of cellular actin assembly. Acta Crystallogr D Struct Biol 2020; 76: 1015-1024.
- [6] Nikolaou S, Juin A, Whitelaw JA, Paul NR, Fort L, Nixon C, Spence HJ, Bryson S and Machesky LM. CYRI-B-mediated macropinocytosis drives metastasis via lysophosphatidic acid receptor uptake. Elife 2024; 13: e83712.
- [7] Chattaragada MS, Riganti C, Sassoe M, Principe M, Santamorena MM, Roux C, Curcio C, Evangelista A, Allavena P, Salvia R, Rusev B, Scarpa A, Cappello P and Novelli F. FAM49B, a novel regulator of mitochondrial function and integrity that suppresses tumor metastasis. Oncogene 2018; 37: 697-709.
- [8] Long Y, Marian TA and Wei Z. ZFR promotes cell proliferation and tumor development in colorectal and liver cancers. Biochem Biophys Res Commun 2019; 513: 1027-1034.

- [9] Zhang Y, Du P, Li Y, Zhu Q, Song X, Liu S, Hao J, Liu L, Liu F, Hu Y, Jiang L, Ma Q, Lu W and Liu Y. TASP1 promotes gallbladder cancer cell proliferation and metastasis by up-regulating FAM49B via PI3K/AKT pathway. Int J Biol Sci 2020; 16: 739-751.
- [10] Li Y, Xiong Y, Wang Z, Han J, Shi S, He J, Shen N, Wu W, Wang R, Lv W, Deng Y and Liu W. FAM49B promotes breast cancer proliferation, metastasis, and chemoresistance by stabilizing ELAVL1 protein and regulating downstream Rab10/TLR4 pathway. Cancer Cell Int 2021; 21: 534.
- [11] Pereira BS, Wisnieski F, Calcagno DQ, Santos LC, Gigek CO, Chen ES, Rasmussen LT, Payão SLM, Almeida RS, Pinto CA, Karia BTR, Artigiani R, Demachki S, Assumpção PP, Lourenço LG, Arasaki CH, Burbano RR, Leal MF and Smith MAC. Genetic and transcriptional analysis of 8q24.21 cluster in gastric cancer. Anticancer Res 2022; 42: 4381-4394.
- [12] Huang H, Tsui YM, Ho DW, Chung CY, Sze KM, Lee E, Cheung GC, Zhang VX, Wang X, Lyu X and Ng IO. LANCL1, a cell surface protein, promotes liver tumor initiation through FAM49B-Rac1 axis to suppress oxidative stress. Hepatology 2024; 79: 323-340.
- [13] Peng P, Zhang W, Cao D, Yang J and Shen K. The proteomic comparison of peripheral circulation-derived exosomes from the epithelial ovarian carcinoma (EOC) patients and non-EOC subjects. Transl Cancer Res 2019; 8: 452-465.
- [14] Hu L, Shen D, Liang D, Shi J, Song C, Jiang K, Menglin Ren, Du S, Cheng W, Ma J, Li S, Bi X, Barr MP, Fang Z, Xu Q, Li W, Piao H and Meng S. Thyroid receptor-interacting protein 13 and EGFR form a feedforward loop promoting glioblastoma growth. Cancer Lett 2020; 493: 156-166.
- [15] Fang K, Du S, Shen D, Xiong Z, Jiang K, Liang D, Wang J, Xu H, Hu L, Zhai X, Jiang Y, Xia Z, Xie C, Jin D, Cheng W, Meng S and Wang Y. SUFU suppresses ferroptosis sensitivity in breast cancer cells via Hippo/YAP pathway. iScience 2022: 25: 104618.
- [16] Jiang K, Yao G, Hu L, Yan Y, Liu J, Shi J, Chang Y, Zhang Y, Liang D, Shen D, Zhang G, Meng S and Piao H. MOB2 suppresses GBM cell migration and invasion via regulation of FAK/Akt and cAMP/PKA signaling. Cell Death Dis 2020; 11: 230.
- [17] Xu H, Liu P, Yan Y, Fang K, Liang D, Hou X, Zhang X, Wu S, Ma J, Wang R, Li T, Piao H and Meng S. FKBP9 promotes the malignant behavior of glioblastoma cells and confers resistance to endoplasmic reticulum stress inducers. J Exp Clin Cancer Res 2020; 39: 44.

- [18] Jiang K, Liu P, Xu H, Liang D, Fang K, Du S, Cheng W, Ye L, Liu T, Zhang X, Gong P, Shao S, Wang Y and Meng S. SASH1 suppresses triplenegative breast cancer cell invasion through YAP-ARHGAP42-actin axis. Oncogene 2020; 39: 5015-5030.
- [19] Zhai X, Shen N, Guo T, Wang J, Xie C, Cao Y, Liu L, Yan Y, Meng S and Du S. SPTLC2 drives an EGFR-FAK-HBEGF signaling axis to promote ovarian cancer progression. Oncogene 2025; 44: 679-693.
- [20] Skirnisdóttir I, Sorbe B and Seidal T. The growth factor receptors HER-2/neu and EGFR, their relationship, and their effects on the prognosis in early stage (FIGO I-II) epithelial ovarian carcinoma. Int J Gynecol Cancer 2001; 11: 119-129.
- [21] Psyrri A, Kassar M, Yu Z, Bamias A, Weinberger PM, Markakis S, Kowalski D, Camp RL, Rimm DL and Dimopoulos MA. Effect of epidermal growth factor receptor expression level on survival in patients with epithelial ovarian cancer. Clin Cancer Res 2005; 11: 8637-8643.
- [22] Gui T and Shen K. The epidermal growth factor receptor as a therapeutic target in epithelial ovarian cancer. Cancer Epidemiol 2012; 36: 490-496.
- [23] Skirnisdottir I, Åkerud H and Seidal T. Clinical significance of growth factor receptor EGFR and angiogenesis regulator VEGF-R2 in patients with ovarian cancer at FIGO stages I-II. Int J Oncol 2018; 53: 1633-1642.
- [24] Forlani L, De Cecco L, Simeon V, Paolini B, Bagnoli M, Cecere SC, Spina A, Citeroni E, Bignotti E, Lorusso D, Arenare L, Russo D, De Angelis C, Ardighieri L, Scognamiglio G, Del Sesto M, Tognon G, Califano D, Schettino C, Chiodini P, Perrone F, Mezzanzanica D, Pignata S and Tomassetti A. Biological and clinical impact of membrane EGFR expression in a subgroup of OC patients from the phase IV ovarian cancer MITO-16A/MANGO-0V2A trial. J Exp Clin Cancer Res 2023; 42: 83.
- [25] Vo D, Liu Y, Sood AK, Rezvani K, Jazaeri AA and Liu J. EGFR, HLA-G, CD70, c-MET, and NY-ES01 as potential biomarkers in high grade epithelial ovarian carcinoma. Cancer Biomark 2024; 39: 289-298.
- [26] Siwak DR, Carey M, Hennessy BT, Nguyen CT, McGahren Murray MJ, Nolden L and Mills GB. Targeting the epidermal growth factor receptor in epithelial ovarian cancer: current knowledge and future challenges. J Oncol 2010; 2010: 568938.
- [27] Wei Y, Erfani S, Schweer D, de Gouvea R, Qadir J, Shi J, Cheng K, Wu D, Craven R, Wu Y, Olivier T, Baldwin LA, Zhou B, Zhou Y, Zhao W, Yang BB, Ueland FR and Yang XH. Targeting receptor

- tyrosine kinases in ovarian cancer: Genomic dysregulation, clinical evaluation of inhibitors, and potential for combinatorial therapies. Mol Ther Oncolytics 2023; 28: 293-306.
- [28] Cooper AJ, Sequist LV and Lin JJ. Third-generation EGFR and ALK inhibitors: mechanisms of resistance and management. Nat Rev Clin Oncol 2022; 19: 499-514.
- [29] Gordon AN, Finkler N, Edwards RP, Garcia AA, Crozier M, Irwin DH and Barrett E. Efficacy and safety of erlotinib HCl, an epidermal growth factor receptor (HER1/EGFR) tyrosine kinase inhibitor, in patients with advanced ovarian carcinoma: results from a phase II multicenter study. Int J Gynecol Cancer 2005; 15: 785-92.
- [30] Schilder RJ, Sill MW, Chen X, Darcy KM, Decesare SL, Lewandowski G, Lee RB, Arciero CA, Wu H and Godwin AK. Phase II study of gefitinib in patients with relapsed or persistent ovarian or primary peritoneal carcinoma and evaluation of epidermal growth factor receptor mutations and immunohistochemical expression: a Gynecologic Oncology Group Study. Clin Cancer Res 2005;11: 5539-48.
- [31] Vergote IB, Jimeno A, Joly F, Katsaros D, Coens C, Despierre E, Marth C, Hall M, Steer CB, Colombo N, Lesoin A, Casado A, Reinthaller A, Green J, Buck M, Ray-Coquard I, Ferrero A, Favier L, Reed NS, Curé H and Pujade-Lauraine E. Randomized phase III study of erlotinib versus observation in patients with no evidence of disease progression after first-line platin-based chemotherapy for ovarian carcinoma: a European organisation for research and treatment of cancer-gynaecological cancer group, and gynecologic cancer intergroup study. J Clin Oncol 2014; 32: 320-6.

- [32] Salinaro J, Singh K, Sands N, Gill V, Perati S, James N, Sharma S, Nasir A, DiSilvestro P, Miller K, Oliver M and Mathews C. Distribution and concordance of HER2 scores in endometrial and ovarian cancer. Gynecol Oncol 2025; 195: 115-121.
- [33] Chen C, Gupta P, Parashar D, Nair GG, George J, Geethadevi A, Wang W, Tsaih SW, Bradley W, Ramchandran R, Rader JS, Chaluvally-Raghavan P and Pradeep S. ERBB3-induced furin promotes the progression and metastasis of ovarian cancer via the IGF1R/STAT3 signaling axis. Oncogene 2020; 39: 2921-2933.
- [34] Sato S, Shintani D, Kaneda Y, Nakamura R, Katoh T, Yano M, Hanaoka M, Yagishita S, Yasuda M, Nagata M and Hasegawa K. Human epidermal growth factor receptor 3 expression in patients with epithelial ovarian cancer: a potential target for ovarian mucinous and clear cell carcinoma. Int J Clin Oncol 2025; 30: 805-813.
- [35] Musacchio L, Valsecchi AA, Salutari V, Valabrega G, Camarda F, Tuninetti V, Giannone G, Bartoletti M, Marchetti C, Pignata S, Fagotti A, Scambia G, Di Maio M and Lorusso D. MEK inhibitor as single agent in low grade serous ovarian and peritoneal cancer: a systematic review and meta-analysis. Cancer Treat Rev 2022; 110: 102458.

